

Performance Evaluation of A Superresolution Algorithm for Image Restoration

C. Bhattacharya, DEAL, India

Abstract:

The class of algorithms called Superresolution is applied to reconstruct signals from apriori known information of limited spectrum and spatial bound of signals. In practice target scene information is limited by aperture point spread function (psf) of sensor and corrupted by noise of the receiving system. Such signal reconstruction is possible only when convex set properties are satisfied with relaxed parameters. A modified Gerchberg algorithm based on Projection Onto convex sets (POCS) with relaxed parameters is presented here with performance analysis for realistic aperture psf characteristic.

I. INTRODUCTION

Images acquired by remotely placed sensors are often limited in quality by poor dynamic range of target reflectivity, finite beamwidth of the aperture of sensor, relative motion between the target and the sensor, etc. Above all, noises present in the background of the scene and generated in the receiving system of the sensor cause loss of information about the scene. Restoration of such images acquired by scanning sensors in non-coherent mode is a topic of active research interest, particularly for sensors working in adverse weather conditions.

The concept of superresolution was formulated by Gerchberg and simultaneously by Papoulis to extract more information of a scene than what is provided by the diffraction limit of the point spread function (psf) of the aperture through so called 'error energy reduction' [1], [2]. Sementelli, et al [3] has broadened the definition of superresolution to include any technique that recovers the signal beyond the cut-off limit of the psf of the imaging sensor. In this sense Gleed and Lettington [4], [5] reported advances in superresolution technique for image restoration using regularized pseudo-inverse of the psf. Several attempts have been made to achieve higher resolution by using superresolution technique on a sequence of low-resolution video frames [6]-[8].

One of the drawbacks of the original Gerchberg algorithm is its very slow rate of convergence after a few initial iterations. The convergence to a solution onto a convex set can be made faster by using relaxed parameter as shown earlier in Schafer et al [9], Levi and Stark [10] and recently in Fahmi [11]. It has been shown in [12] that using Projection Onto Convex Set (POCS) technique with relaxed parameters, fast convergence of iteration is possible with noisy images.

This paper is on the performance of a modified Gerchberg algorithm using relaxed parameters for restoration of images collected in scanning sensor scenario. Performance of superresolution techniques is often evaluated on images modelled with ideal aperture profile causing confusion on signal reconstruction beyond diffraction limit. A brief overview of the concept of superresolution with one-dimensional signal is given in section II. In section III we present the modified Gerchberg Algorithm; simulation results are provided for performance analysis of the algorithm in section IV. Section V draws the conclusion of the paper.

II. SIGNAL RECOVERY BEYOND DIFFRACTION LIMIT (SUPERRESOLUTION)

Considering a linear shift invariant model of the imaging sensor, the received signal, \mathbf{g} may be expressed as,

$$\mathbf{g} = \mathbf{H} \mathbf{f} + \mathbf{n} , \quad (2.1)$$

where \mathbf{f} is the signal representing target scene reflectivity, \mathbf{H} is the psf of the aperture of the sensor and \mathbf{n} is the Gaussian noise of the receiving sensor. Approximation of the target scene, $\hat{\mathbf{f}}$ from equation (2.1) is then an inverse problem; solution of which within ω_c , the cut-off limit of the spectrum of the psf, is given by deconvolution using pseudo-inverse of the function \mathbf{H} . The restored signal, $\hat{\mathbf{f}}$ has the same cut-off, ω_c as that of the aperture psf. As shown in figure 2.1(a) and (b), superresolution is reconstruction of the signal beyond ω_c , incorporating higher frequencies in the spectrum of $\hat{\mathbf{f}}$ and hence achieving better spatial resolution.

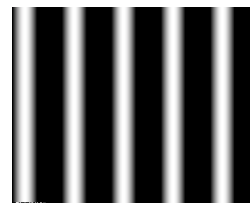


Fig.2.1(a) Low frequency Sinusoid Basis Vector

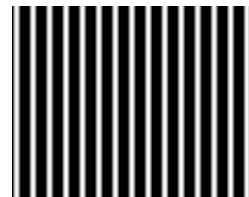


Fig.2.1(b) High frequency Sinusoid Basis Vector

Such signal reconstruction is possible only when \mathbf{g} and \mathbf{f} are

members of the intersection of convex sets, \mathbf{C}_I and \mathbf{f}^\wedge converges to a solution within this intersection, \mathbf{C}_0 , given by,

$$\mathbf{C}_0 = \bigcap_{i=1}^m \mathbf{C}_i$$

The convex sets \mathbf{C}_i represent the constraints on the signal, both in spatial and spectrum domain. After n iterations, the solution of this POCS technique is given by,

$$\mathbf{f}^\wedge_n = P_{m,n} P_{m-1,n} \dots P_{1,n} \mathbf{g}, \quad (2.2)$$

where $P_{i,n}$ is the projection operator on the i th convex set \mathbf{C}_i after n iterations.

In the original Gerchberg-Papoulis algorithm only two projection operators are used; i.e. positivity constraint of the signal in the spatial domain and *a priori* known spectrum in the frequency domain.

Equation (2.2) is then given as,

$$\mathbf{f}^\wedge_n = P_{2,n} P_{1,n} \mathbf{g} \quad (2.3)$$

The convergence to a solution in \mathbf{C}_0 may be made faster by using relaxed parameter. The new projection operator may be given as,

$$T_i = (1 - \alpha_i)I + \alpha_i P_i \quad (2.4)$$

where I is the identity operator and the bound on the relaxed parameter, α_i is, $1 < \alpha_i < 2$, [11].

The result of this POCS technique for superresolution of one-dimensional signals is shown in figures 2.2(a), (b).

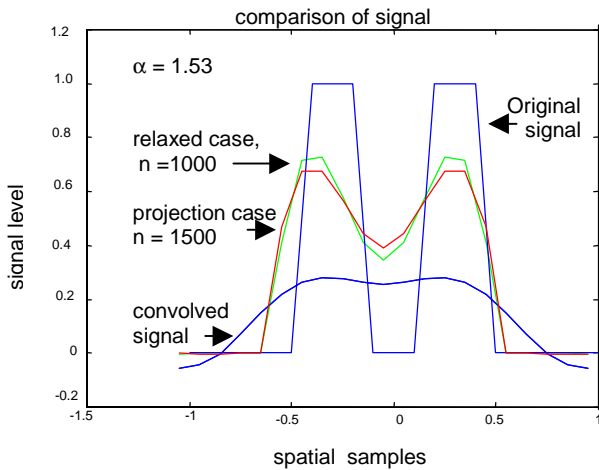
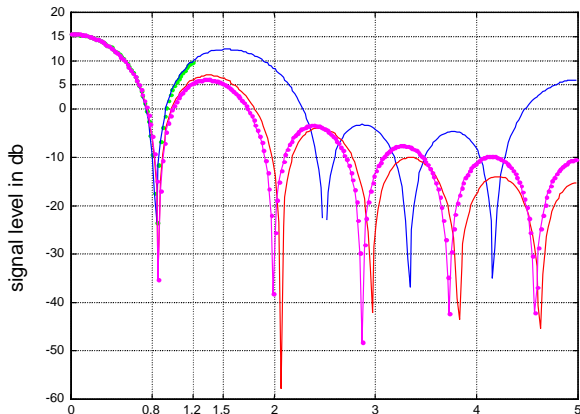


Fig.2.2(a), Superresolution in 1-D
comparison of signal power spectrum



spatial frequencv. $F_s = 10\text{cycles/rad}$

Fig.2.2(b), Spectral extrapolation in 1-D

Filter cut off : 1.2 cycles/rad, brick wall function

Spectrum used: 0.8cycles/rad, $\alpha = 1.53$

Legend :

- color blue : original signal power spectrum
- color green : convolved signal power spectrum
- color red : superresolution with relaxed parameter, $n = 1000$
- color magenta : superresolution with only projection operator, $n = 1500$

In figure 2.2 (a) an ideal target, two spikes separated by 0.2 units of distance represent \mathbf{f} . The aperture psf is a brickwall function in the spectral domain with spectral cutoff at 0.12 of sampling frequency, f . The spectra of signals, \mathbf{f} , \mathbf{g} , \mathbf{f}^\wedge after $n = 1500$ iterations of the algorithm in equation (2.3) are shown in figure 2.2(b). The spectrum extrapolation of the reconstructed signal, \mathbf{f}^\wedge will lead to much higher sharpness in the spatial domain as shown in figure 2.2 (a). Using the relaxed projection operator in the spatial domain, described in section III, the number of iterations n can be made 1000 as shown by the green color in figure 2.2(a). Since the POCS technique operates linearly on signal and noise, noise reduction after n iterations is evident and is shown in [12]. The error in approximation, $\|\mathbf{f}_n^\wedge - \mathbf{f}\|$ saturates as n becomes larger and is shown in figure 2.3.

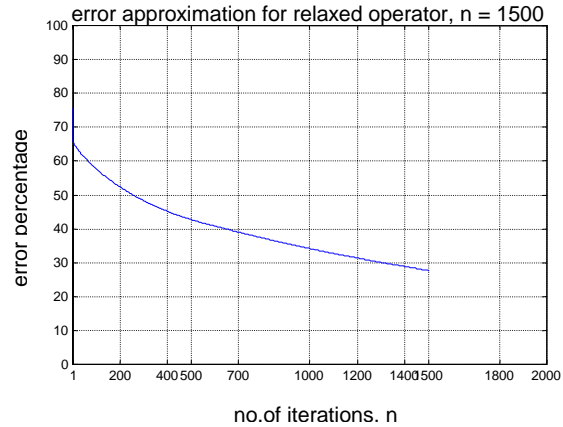


Fig.2.3, Approximation error vs. n

III. MODIFIED GERCHBERG ALGORITHM

In actual scenario, the spectrum of \mathbf{f} is not known *a priori* and the psf is not a brickwall function. For a scanning sensor, the psf in equation (2.1) represents an one-dimensional convolution operator, $h(i,j)$ and the imaging sensor model may be given by,

$$\mathbf{g}(x, j) = \sum_{x=1}^N h(x-i, j) \mathbf{f}(i, j) + \mathbf{n}(x, j), \quad (3.1)$$

where (x, j) represent the discrete positions of scanning.

Hence,

$$G(\omega_1, \omega_2) = H(\omega_1, \omega_2) \otimes F(\omega_1, \omega_2) \quad (3.2)$$

in the spectral domain. Here \otimes represents circular convolution operator and additive noise may be skipped without loss of generality of assumptions. Since the data size and the psf kernel size are large, convolution is done in spectral domain.

The spectrum of \mathbf{f} as is given in equation (3.2) is not only altered by the magnitude weight of $H(\omega_1, \omega_2)$ but also by the phase function $\phi_H(\omega_1, \omega_2)$. If we consider $h(i, j)$ to be of narrow beamwidth as is shown in figure 3.1(a), its spectrum is sufficiently flat in the low frequency zone as is shown in figure 3.1(b).

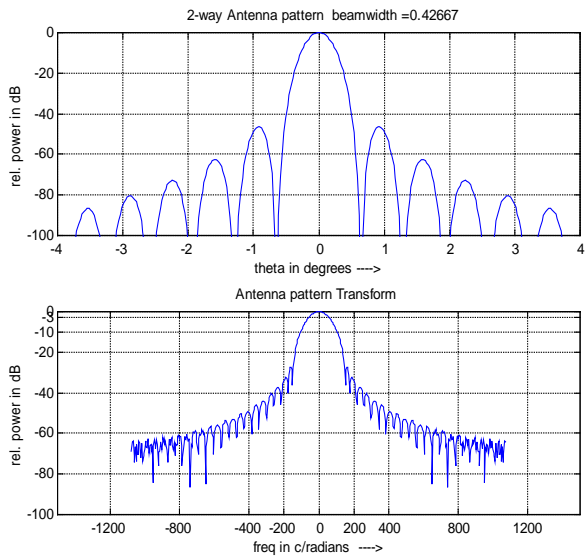


Fig.3.1 (a), (b), Aperture gain pattern and its Transform

To approximate the spectrum of $F(\omega_1, \omega_2)$ from $G(\omega_1, \omega_2)$ in this low frequency zone, phase alteration by $\phi_H(\omega_1, \omega_2)$ may be compensated by modifying equation (3.2) as,

$$G'(\omega_1, \omega_2) = G(\omega_1, \omega_2) \cdot e^{-j(\phi_H(\omega_1, \omega_2))}, \quad (3.3)$$

where $G'(\omega_1, \omega_2)$ is the phase compensated spectrum of $g(i, j)$. A signal dependent co-efficient, $\xi(j)$ is used to compensate the magnitude weighting of $H(\omega_1, \omega_2)$.

$$\text{Thus, } G''(\omega_1, \omega_2) = \xi(j) * G'(\omega_1, \omega_2), \quad (3.4)$$

where $\xi(j)$ is the co-efficient, dependent on the dynamic range of the signal, $g'(i, j)$, in the low frequency zone.

Using the spatial domain signal, $g''(i, j)$ and low frequency spectrum of $G''(\omega_1, \omega_2)$, the iterations of the relaxed POCS method follows.

The flow of the iterations is shown in figure 3.2.

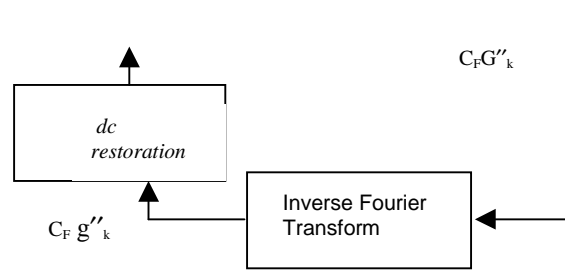
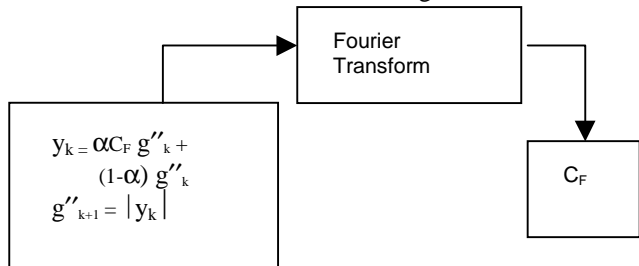


Fig.3.2, Flow of modified Gerchberg Algorithm

Considering the k th iteration, the algorithm starts from the k th estimate, g''_k in the space domain. The Fourier domain constraint, C_F as represented by the low frequency spectrum of $G''(\omega_1, \omega_2)$ in equation (3.4) is applied on the Fourier transform of the image, G''_k .

The projection operator applied to the inverse Fourier transform is given as, g''_{k+1} ,

$$y_k = \alpha C_F g''_k + (1-\alpha) g''_k \quad (3.5)$$

$$g''_{k+1} = |y_k| \quad (3.6)$$

Apart from the constraints as given in equation (3.5) and (3.6), we also use the dc constraint as for the actual target scenes, most of the signal energy is contained in the dc term of the spectrum.

After n iterations, the approximation, \mathbf{f}^\wedge is given as,

$$\mathbf{f}^\wedge = g''_{n+1} \quad (3.7)$$

IV. PERFORMANCE ANALYSIS

For analyzing the performance of the algorithm presented in section III we use a narrow beamwidth (0.4 deg.) aperture psf, the gain pattern and transform of which are given in figure 3.1(a) and (b). For the spread of the psf, we take five sidelobes on each side of the gain pattern. The target image, \mathbf{f} is shown in figure 4.1(a) as the strip of a blood cells image. This image is convolved in column direction only and blurred sufficiently by taking out all powers below 0 db and is shown in figure 4.1(b) as the signal, \mathbf{g} .

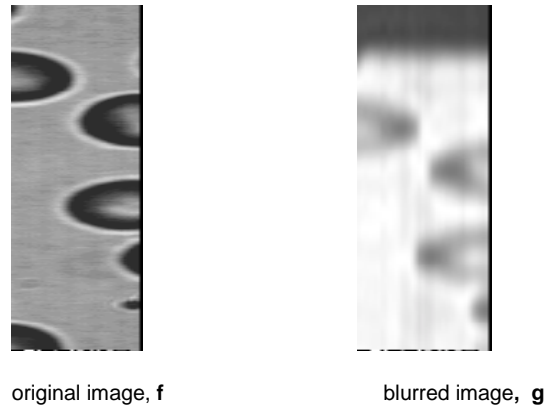


Fig.4.1(a)

Fig.4.1(b)

knowledge of the psf of the aperture of the sensor and the mode of scanning in the acquisition process.

Acknowledgement: The author acknowledges the suggestions from reviewers. Thanks for the encouragement received from Capt.(IN)P. Shukla (Retd.) to complete the work. The kind permission of Director, DEAL to submit the work is gratefully acknowledged.

Phase shifted
Image, g'

Superresolved
Image, f_n^* , $n = 1000$

Fig.4.1(c)

Fig.4.1(d)

The phase compensated version, g' is shown in figure 4.1 (c). After $n = 1000$ iterations of the algorithm given in figure 3.2, the resultant approximation is shown in figure 4.1 (d).

It is seen from figure 4.1 (a) and 4.1(b), that apart from blurring, the effect of psf pattern is to alter the phase of the image. This is because the dimension of the convolved function increases by $(M-1)$ points, where M is dimension of the gain pattern vector. Taking this into account, the phase compensated image in figure 4.1(c) represents a blurred version of the target image.

For estimating the error in approximation, we use the measure of mean distance and variance of distance of approximation, $\|f_n^* - f\|$, [10]. The measures are given in table I.

TABLE –I

$n = 1000$; $\alpha = 1.95$

Function	Mean Distance, $d_{mean} =$ $mean(\ f_i - f\)$	Variance Distance, $d_{var} =$ $var(\ f_i - f\)$	Error in % = $d_{var}/$ $var(f)$
g (Fig. 4 (b))	0.3264	0.0217	82.36%
g' (Fig. 4(c))	0.2706	0.0101	62.05%
f_n^* (Fig. 4 (d))	0.1121	0.0042	37.74%

V. CONCLUSION

From the table of performance analysis it can be seen that the Superresolution technique of modified Gerchberg algorithm can be used to restore sharpness and texture information of a blurred image in a realistic scenario. For this accurate estimation of the low frequency spectra of target scene is necessary. This can be achieved with reliable

References

1. Gerchberg R W , 1974, “ Super-resolution through error energy reduction”, Optica Acta, 21, 709 –720
2. Papoulis A, 1975, “ A new algorithm in spectral analysis and bandlimited extrapolation”, IEEE Trans. Circuits Syst., CAS-22, 735-742
3. Sementilli P J, Hunt B R, Nadar M S, 1993, “ Analysis of the limit to superresolution in incoherent imaging”, J.Opt.Soc.Am.A, 10, 2265-2276
4. Gleed D G and Lettington A H, 1991, “ Application of superresolution techniques to passive millimetre-wave images”, SPIE , 1567, 65 - 73
5. – DO - , 1994, “ High speed superresolution technique for passive millimetre-wave imaging systems”, SPIE, 2182, 255-259
6. Elad M and Feuer A, 1997, “ Restoration of a Single Superresolution Image from Several Blurred, Noisy, and Undersampled Measured Images”, IP (6), No. 12, pp. 1646-1658.
7. –DO-, 1999, “ Super-Resolution Reconstruction of Image Sequences”, PAMI(21) No. 9, pp. 817.834.
8. –DO-, 1999, “ Superresolution Restoration of an Image Sequence: Adaptive Filtering Approach”, IP(8) No. 3, pp. 387.
9. Schafer R W, Mersereau R M , Richards M A, 1981, “ Constrained Iterative Restoration Algorithms”, Proc.IEEE, 69(4), 432 – 450
10. Levi A and Stark H, “Restoration from Phase and Magnitude by Generalized Projections “, in H. Stark ed. ,1987 , “ Image Recovery – Theory and Applications”, Academic press, ch. 8, pp 277 – 320
11. Fahmi H , “ A fast new approach to super-resolution”, SPIE, 2564, 117 – 124
12. Bhattacharya C and Shukla P, 1999, “ A Fast Adaptive Superresolution technique for Image Restoration”, IPA'99, Pub.No.465, IEE, pp.827-831

